Chemical bath deposition of thin film CdSe layers for use in Se alloyed CdTe solar cells

Kerrie M. Morris, Christos Potamialis, Francesco Bittau, Jake W. Bowers and John M. Walls

Centre for Renewable Energy Systems Technology (CREST), Wolfson School of Mechanical, Electrical and Manufacturing Engineering, Loughborough University, Loughborough, Leicestershire, LE11 3TU, UK

***Abstract* — Chemical bath deposition (CBD) was used as a method to deposit CdSe thin films for use in CdTe solar cells. Solution parameters such as precursor stoichiometry, concentration and deposition time, were varied to assess the impact on the morphology of the CdSe films deposited on FTO coated glass. The solution precursors were cadmium acetate and sodium selenosulphite with NH_3 used as a complexant to control the release of ions into the solution. It was seen that particle size, surface coverage and thickness were successfully controlled. CdSe films were grown with a band gap of ~1.74 eV and were made into full devices with CdTe. A ternary compound of $CdTe_{1-x}Se_x$ formed with a band gap of ~1.40 eV, which was shown in an improved EQE in the IR, as well as an improved Jsc. The best device, with an efficiency of 12.3% was produced from a 280 nm thick film with a surface coverage of 59% and grain size of ~600 nm. An increased response at longer wavelengths due to the lowered band gap resulted in a high J_{SC} value of 28.2 mA cm^{-2} suggesting efficient intermixing of the CdSe into the $CdTe_{1-x}Se_x$ layer.**

***Index Terms* — Cadmium compounds, photovoltaic cells, selenium, surface morphology, thin film devices.**

I. Introduction

Cadmium telluride (CdTe) thin film photovoltaics (PV) currently have a power conversion efficiency (PCE) of 22.1% [1]. CdTe is a direct band gap semiconductor of ~1.5 eV with a theoretical maximum PCE of almost 33% [2]. Since CdTe heterojunction devices have not yet reached their maximum potential, the scope for improvement of the PCE coupled with low-cost fabrication ensures this remains a viable research area. An improvement in efficiency could be achieved by lowering the material band gap which would enable conversion of a larger fraction of the infrared (IR) spectrum [3]. Doping CdTe with selenium (Se) forms a ternary compound ($CdTe_{1-x}Se_x$). This results in a bowing of the band gap [4] which reduces the band gap of unalloyed CdTe and can also increase the minority carrier lifetime of the alloy [5].

Two main strategies to incorporate selenium in CdTe solar cells exists. The first consists of including a cadmium selenide (CdSe) layer in the solar cell structure, adjacent to the CdTe absorber [6]–[8]. CdSe is an n-type semiconductor with a band gap of ~1.74 eV [9]. CdSe can diffuse into the CdTe layer during high temperature annealing, which forms a $CdTe_{1-x}Se_x$ alloy. This ternary compound exhibits a band gap of 1.36 eV [7] with a composition of $CdTe_{0.6}Se_{0.4}$ [4]. Consequently, the amount of intermixing which occurs depends upon the thickness of the initial CdSe layer and how effective the inter-diffusion between the CdSe and the CdTe layer is. This effect can result in a fully consumed CdSe layer which would require a large band gap buffer layer such as tin oxide to form the p-n junction or to include a CdS layer as the n-type semiconductor. Another method involves the co-sublimation of a Se source with CdTe, to form $CdTe_{1-x}Se_x$ [10], [11] during the deposition process. In both methods, band gap grading can occur which, if controlled correctly, can lead to a favorable electric field distribution throughout the absorber bulk and can lead to an increased open circuit voltage (V_{oc}) [10]. Chemical bath deposition (CBD) is used as a simple method to deposit CdSe layers, to incorporate into CdTe solar cells, to form the narrow band gap $CdTe_{1-x}Se_x$ alloy [6], [7]. CBD offers a scalable, atmospheric, low-cost route for the fabrication process.

In this study cadmium acetate ($Cd(CH_3COO)_2$) and sodium selenosulphite (Na_2SeSO_3) have been used as Cd^{2+} and Se^{2-} ion sources, respectively. The film uniformity, film thickness and deposition rate on the FTO coated substrate are highly dependent on the rate the ions are released into the bulk solution [12]. The release of the ions only occurs when the ionic product is greater than the solubility product and a uniform thin film is only seen when this is carefully controlled [13]. If the ion release is not controlled then local precipitation can occur within the chemical bath rather than on the substrate. Cadmium acetate fully dissociates in water and complexing the Cd^{2+} ion with ammonia (NH_3), as shown in (2) controls the ion release [14]. Ammonia is added in the form of ammonium hydroxide (NH_4OH) as it hydrolyses in water according to (1). The hydroxide ion (OH^-) is also an integral part to the reaction as seen in (3) as the release of Se^{2-} depends on this [14].

$$NH_3 + H_2O \leftrightarrow NH_4^+ + OH^- \quad (1)$$

$$Cd^{2+} + 4NH_3 \leftrightarrow Cd(NH_3)_4^{2+} \quad (2)$$

$$Na_2SeSO_3 + 2OH^- \rightarrow Na_2SO_4 + H_2O + Se^{2-} \quad (3)$$

Changing the bath parameters such as complexant, temperature and pH has been shown to offer some control over whether a zinc-blende type structure (cubic), wurtzite type structure (hexagonal), or both, are formed [13], [15]. CdSe exhibits a hexagonal structure as the stable phase, which predominantly forms during deposition steps during standard processing steps such as annealing and $CdCl_2$ treatment, the

CdSe layer diffuses and is converted to a $CdTe_{1-x}Se_x$ cubic structure [16]. CBD optimisation of the CdSe therefore is a key step within the fabrication process of $CdTe_{1-x}Se_x$ solar cells, as a means to improve device efficiency by focusing on improving film uniformity, thickness and crystal structure.

II. Experimental procedure

A. CdSe Deposition Procedure

CdSe thin films were prepared on TEC™ 12D low iron glass substrates (Pilkington, F-doped tin oxide, tin oxide buffer layer, coated glass) by CBD containing solutions of cadmium acetate and sodium selenosulphite. The cadmium acetate solution was prepared by adding cadmium acetate powder to 20 ml deionized (DI) water and mixing until dissolved. The sodium selenosulphite stock solution was prepared by adding sodium sulfite (Na_2SO_3) and selenium powder (Se) into a flask containing 20 ml DI water at a 10:1 stoichiometry of sodium sulphite to selenium as this aided the dissolution of selenium into solution. This was maintained at 85 °C for 2 hours under stirring. The solution was then cooled, filtered and used within 24 hours. The deposition bath was prepared in a beaker by adding 200 ml of DI water at 88°C. The reactants were added in the following order, cadmium acetate solution, ammonium hydroxide and sodium selenosulphite solution and the volume topped up to 275 ml with DI water. The pH was measured at >13. The FTO coated glass substrates were inserted vertically near the beaker wall and the temperature of the bath was kept at 88°C under stirring, for varying durations. At the end of the deposition, the substrates were removed from the bath and rinsed with DI water and dried. The deposition duration, stoichiometry and concentration of reactants were varied to assess the effect on film thickness and quality.

B. Chemical Bath Deposition Optimisation

Firstly, a 1:1 stoichiometric solution of cadmium acetate (1 mmol) and sodium selenosulphite (1 mmol) was investigated with 10 ml of ammonium hydroxide, for a 2 hour deposition time. Within 3 minutes of the precursors being added to the chemical bath, the solution was seen to rapidly change from a clear colourless solution to a dark brown, opaque solution. On removal of the substrates, an uneven chalky film was seen which suggested the ion release was too rapid and local precipitation within the solution occurred. The volume of ammonium hydroxide was then increased to 15ml, and a more uniform film with no chalky residue was achieved.

The precursor concentration and stoichiometry were then varied as per Table I. The concentration was increased by increasing the amount of reactants in the chemical bath, whilst keeping the volume of solution constant. The CBD recipe that gave the thickest film was then repeated with increased deposition time of 4 hours and 6 hours. The volume of ammonium hydroxide was increased in line with the amount of cadmium acetate, so the rate of release of Cd^{2+} ion would not change as a function of ammonium hydroxide concentration.

TABLE I
CBD PRECURSOR COMPOSITION

Reference	Amount Cd^{2+} (mmol)	Amount Se^{2-} (mmol)	Deposition Time (hrs.)
2 hr (1:1 mmol)	1	1	2
2 hr (2:2 mmol)	2	2	2
2 hr (1:2 mmol)	1	2	2
2 hr (2:4 mmol)	2	4	2
4 hr (2:4 mmol)	2	4	4
6 hr (2:4 mmol)	2	4	6

C. Device Fabrication

CdTe deposition was carried out in a home-made close space sublimation (CSS) system. Source and substrate temperatures were kept at 630°C and 515°C respectively, at a separation of 2 mm. The reactor was filled with a 6% O_2 in Ar gas mixture, at a pressure of 1 Torr. The deposition time was 3 minutes, which resulted in 2-4 µm thick films. The $CdCl_2$ activation treatment was carried out by thermal evaporation and subsequent annealing. A quartz crucible was loaded with 0.5 g of $CdCl_2$ pellets, which was then evaporated at ~1 x 10^{-6} Torr for 20 minutes. The sample was then annealed on a hot plate at a dwell temperature of 450°C for 1 minute, with a ramping rate of 22°C/minute. Devices were rinsed with DI water to remove any $CdCl_2$ residue and the cell was completed with 85 nm gold contacts deposited using thermal evaporation.

D. Characterization

The optical properties of the films were investigated using a Varian Cary 5000 UV-VIS-NIR spectrophotometer. The structural properties of the films were analysed by X-ray diffraction (XRD) using a Brucker D2 phaser desktop X-ray diffractometer equipped with a Cu-K-alpha X-ray gun. The XRD measurements were obtained using 15 rpm rotation, a 1mm beam slit and 3mm anti-scatter plate height. The film surface morphology was imaged with a JSM-7800F Schottky Field Emission Scanning Electron Microscope (SEM). Surface area coverage was analysed using image processing in MATLAB. The film thickness of each sample was measured using an Ambios XP-2 profilometer. The current density-voltage (JV) characteristics of devices were determined using a bespoke solar simulator under a simulated AM1.5G spectrum. External quantum efficiency (EQE) measurements were carried out using a PVE300 EQE system (Bentham Instruments Limited, UK) with a 5 nm resolution.

III. RESULTS AND DISCUSSION

A. Thin Film Morphology

The SEM image [2 hr (1:1 mmol)] seen in Fig. 1. illustrates CdSe clusters nucleating over the surface of the FTO. The nucleation process follows the steps of the Volmer–Weber growth mode, with the nucleation centres forming islands which progressively grow in size and density as can be seen in the samples with longer a longer deposition time [6 hr (2:4 mmol). Samples [2 hr (1:1 mmol)] to [2 hr (2:2 mmol)] saw a doubling of the cadmium and selenium precursor concentration as shown in Table I, which resulted in a similar particle size of 100 – 300 nm, but increased surface area coverage from 10 – 13%. From [2 hr (1:1 mmol)] to [2 hr (1:2 mmol)] where only the concentration of the Se was doubled, a similar particle size of 100 – 300 nm was observed but an increased surface area coverage was seen up to 20%. Doubling the concentration from [2 hr (1:2 mmol)] to [2 hr (2:4 mmol)] resulted in a wider ranging nucleation size of 50 – 300 nm and a significantly increased surface area coverage of >80%.

Subsequently, the deposition time was then increased to 4 hours [4 hr (2:4 mmol)] whilst keeping the same concentration and stoichiometry, which produced a wide surface area coverage of 59%. The increased deposition time also resulted in much larger particle sizes of 500 – 800 nm. With an increased deposition time of 6 hours [6 hr (2:4 mmol)], the particle size further increased to 700 – 1000 nm, with a surface area coverage of 65%.

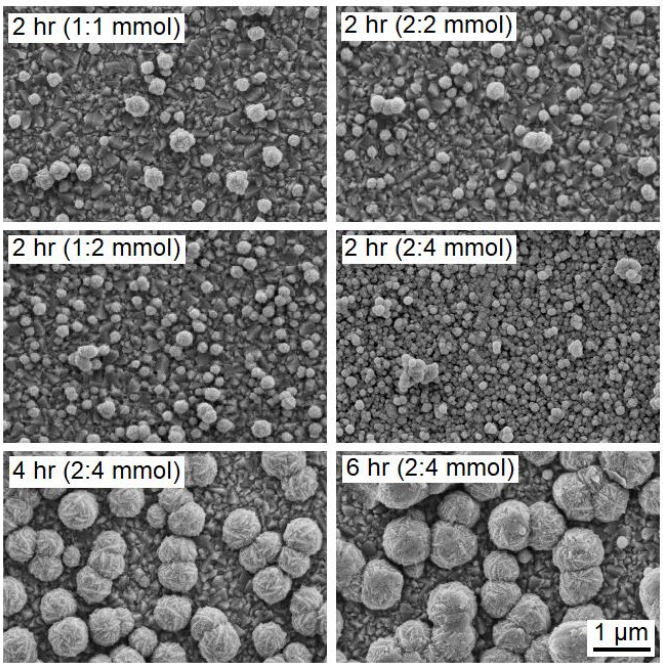

Fig. 1. SEM images of as-deposited CdSe thin films at varying stoichiometries (Cd:Se) and varying deposition times.

These results indicate that a 1:2 stoichiometry and higher concentrations result in an increased surface coverage and hence a more uniform film. Increasing the deposition time from 2 hours then results in the particle size increasing. Increased surface coverage and particle size results in thicker films, as shown in Table II.

TABLE II
MORPHOLOGY OF THIN FILMS

Reference	Thickness (nm)	Surface coverage (%)
2 hr (1:1 mmol)	110	10
2 hr (2:2 mmol)	150	13
2 hr (1:2 mmol)	160	20
2 hr (2:4 mmol)	175	>80
4 hr (2:4 mmol)	280	59
6 hr (2:4 mmol)	340	65

B. Structural Analysis

Fig. 2. shows *X*-ray diffraction (XRD) patterns of the investigated samples. Analysis shows a hexagonal CdSe structure with peaks at 2Θ values of 24.5º, 25.7º, 42.6º and 49.9º which correspond to (100), (002), (110) and (112) reflections (PDF # 08-0459). The thinner films have a low peak intensity, which does increase with increasing thickness, nonetheless the XRD indicates a clear CdSe growth. The strongest peak attributed to the CdSe film suggests orientation along the (002) plane [17].

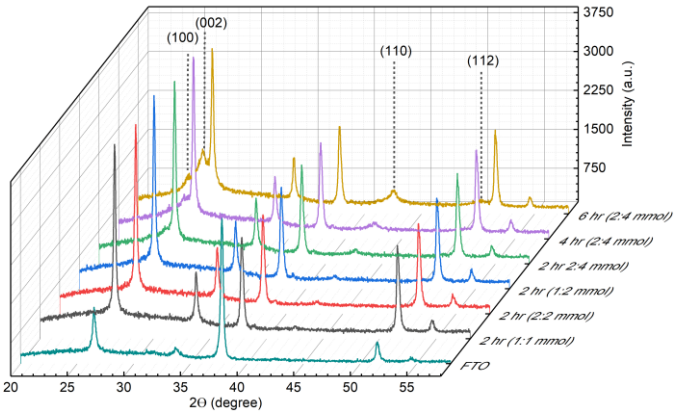

Fig. 2. The XRD patterns of the as-deposited CdSe thin films.

The remaining peaks seen are due to the FTO coated substrate [18] which is shown in Fig. 2 as reference peaks, the FTO peaks remained constant at increasing thicknesses.

C. Optical Properties

The transmission spectra of the CdSe thin films are shown in Fig. 3. An absorption onset at ~680 nm can be seen which corresponds approximately to the CdSe band gap of 1.75 eV. As the thickness of the film increases, the transmission

decreases and the band gap onset is sharper due to a thicker film absorbing a greater proportion of light.

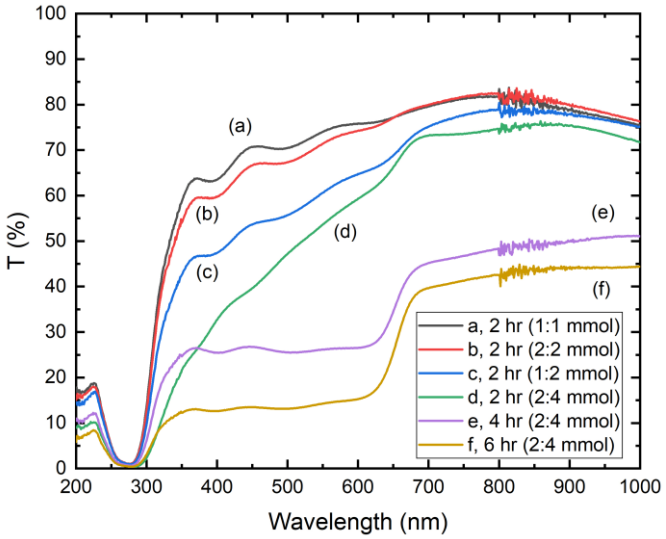

Fig. 3. The transmission spectra of the as-deposited CdSe films.

A Tauc plot of $(\alpha hv)^2$ vs hv, [19] where α was calculated from transmittance data, was used to estimate the band gaps. As shown in Fig. 4. the linear part of the graph was extrapolated and the band gap for each thin film was determined.

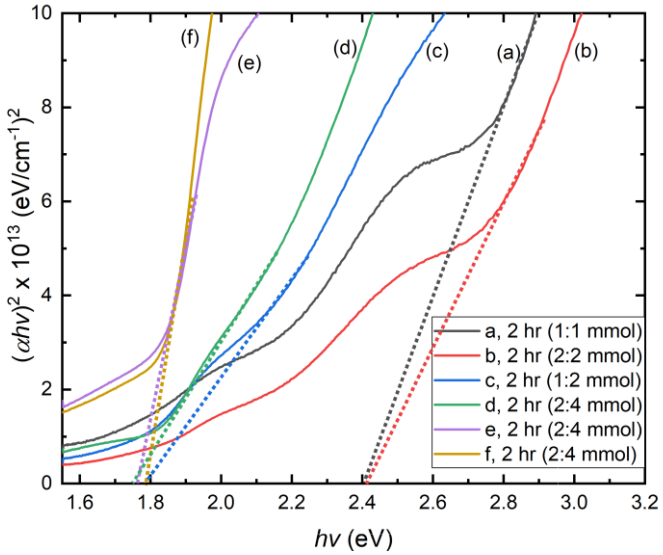

Fig. 4. Plots of $(\alpha hv)^2$ vs hv for the as-deposited CdSe thin films.

For [2 hr (1:1 mmol)] to [2 hr (2:2 mmol)] the Tauc plot was difficult to extrapolate due to the high transmission and shallow absorption onsets and interference fringes seen on the transmission spectra, however for clarity, each plot has been shown. From the analysis, these thinner films present band gaps of 2.4 eV, which as previously discussed is likely erroneous due to the films being too thin. The remaining samples [2 hr (1:2 mmol)], [2 hr (2:4 mmol)], [4 hr (2:4 mmol)] and [6 hr (2:4 mmol)], which had a sharper absorption onset, all gave a band gap of ~1.75 eV which was anticipated for CdSe [9]. A summary of band gaps of each film is listed in Table III.

The films with a band gap ~1.75 eV were then made into complete devices to assess the performance of Se alloyed CdTe solar cells. The thinner films with higher band gaps (2.4 eV) were omitted from further device fabrication.

D. Full Device Analysis

Table III shows the best performing cell for each of the completed CdSe films, with the corresponding J-V and EQE curves in Fig. 5 and Fig. 6 respectively. The small particle size and similar thickness of [2 hr (1:2 mmol)] and [2 hr (2:4 mmol)] gave a similar efficiency of 10.3% and 10.5% respectively. [2 hr (2:4 mmol)] had a slight increase in V_{OC} of 679 mV compared to [2 hr (1:2 mmol)] V_{OC} of 658 mV but a lower J_{SC} and FF.

For the two films deposited for 2 hours, and the film deposited for 4 hours, the EQE shows an initial sharp increase at shorter wavelengths, corresponding to the band gap of the SnO_2 buffer layer. No parasitic absorption is observed at short wavelengths, indicating complete diffusion of the CdSe layer into the CdTe. With increasing CdSe film thickness, there is a clear improvement in EQE at longer wavelengths, especially for [4 hr (2:4 mmol)], indicating a band gap shift to 1.39 eV, Fig. 7. shows the band gaps extracted from the EQE data.

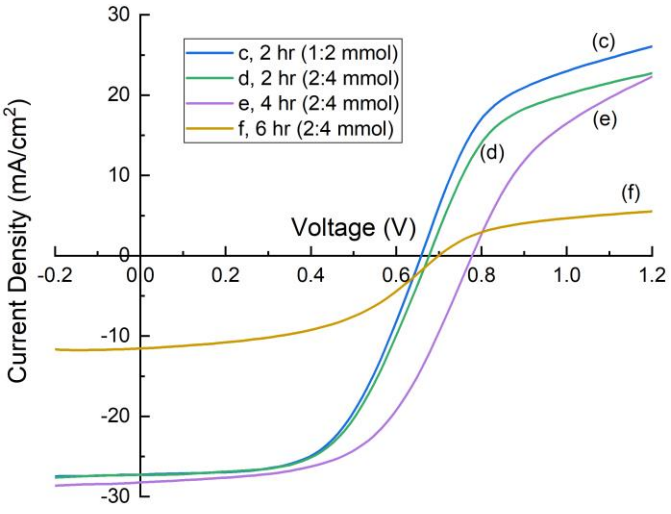

Fig. 5. J-V curves for the CdSe/CdTe devices fabricated.

[6 hr (2:4 mmol)] exhibited a much larger response in the longer wavelengths compared to [2 hr (1:2 mmol)] and [2 hr (2:4 mmol)] but shows an almost 50% reduction in EQE across all wavelengths when compared to the other devices, hence a comparatively low J_{SC} of only 11.5 mA cm^{-2} was produced.

TABLE III

EFFICIENCY (η), SHORT CIRCUIT CURRENT DENSITY (J_{SC}), OPEN CIRCUIT VOLTAGE (V_{OC}), AND FILL FACTOR (FF) AS A FUNCTION OF CdSe CBD PARAMETERS AND THIN FILM CHARACTERISTICS

Reference	Thickness (nm)	Surface coverage (%)	Band gap of CdSe film (eV)	Band gap of device (eV)	η (%)	J_{SC} (mA cm^{-2})	V_{OC} (mV)	FF (%)
2 hr (1:2 mmol)	160	20	1.78	1.46	10.3	27.2	658	57.4
2 hr (2:4 mmol)	175	>80	1.76	1.48	10.5	27.3	679	56.9
4 hr (2:4 mmol)	280	59	1.76	1.39	12.3	28.2	778	56.0
6 hr (2:4 mmol)	340	65	1.78	1.38	4.8	11.5	701	47.6

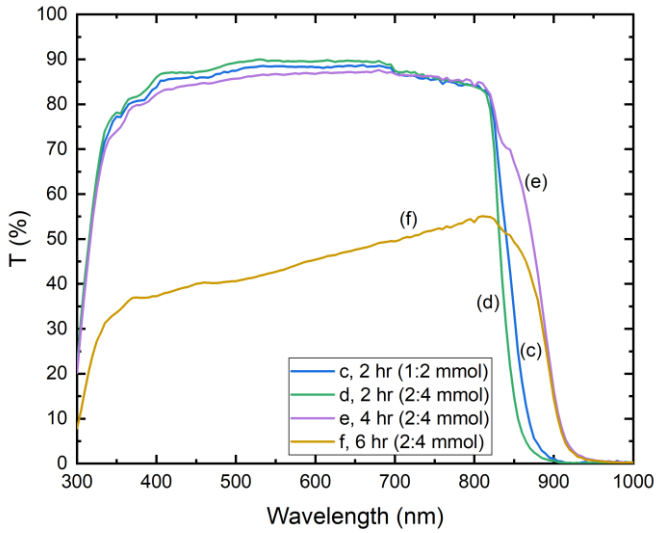

Fig. 6. EQE data for the CdSe/CdTe devices fabricated.

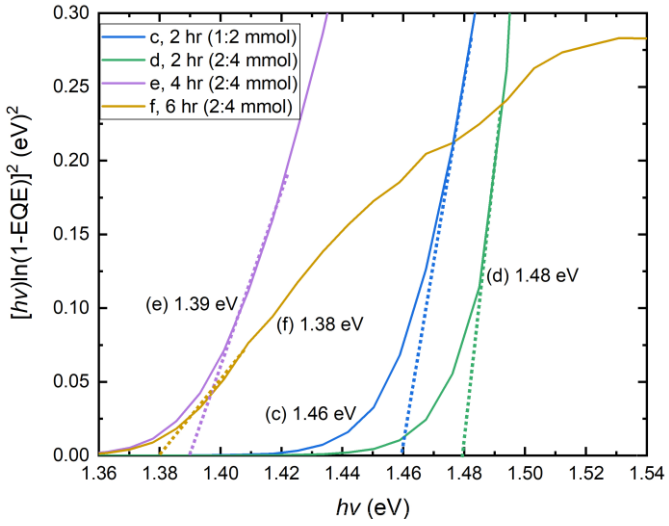

Fig. 7. Band gap data extracted from the EQE data in Fig. 6

Combined with the lowest FF of 47.6 %, this device gave an overall efficiency of 4.8%. The low EQE may be the result of a thicker CdSe layer remaining after the $CdCl_2$ treatment, which resulted in parasitic light absorption at shorter wavelengths.

The low response at longer wavelengths may be due to an unoptimized junction formation between the CdSe and the $CdTe_{1-x}Se_x$.

[4 hr (2:4 mmol)] with an efficiency of 12.3% had the highest V_{OC} at 778 mV and J_{SC} at 28.2 mA cm^{-2} and a FF of 56.0%. The EQE showed a slightly reduced response compared to [2 hr (1:2 mmol)] and [2 hr (2:4 mmol)], however the increased response up to 950 nm improved the Jsc slightly. The high V_{OC} of 778 mV [4 hr (2:4 mmol)] suggested that of all the devices this formed the best SnO_2 buffer\$CdTe_{1-x}Se_x$ interface. The low FF can be attributed to a unoptimized back contact, since only gold was used, and no intentional copper was added to back contact.

IV. CONCLUSION

This study has shown that CBD of CdSe can produce device quality films that are suitable for incorporation into CdTe solar cells. Varying the concentrations of reactants and/or stoichiometry along with deposition time can be used to change the morphology of the film at the nanoscale level, i.e. particle size and coverage which has been seen to affect the efficiency of the completed CdSe/CdTe device. Only the wurtzite type structure was identified in this study, but this was successfully coupled with a CdTe layer to give moderate efficiencies.

The best device was formed, with an efficiency of 12.3%, from a 280 nm thick CdSe film with a surface coverage of 59%. This resulted in an optimal diffusion of the CdSe into the CdTe to form the ternary compound $CdTe_{1-x}Se_x$. The highest J_{SC} and V_{OC} at 28.2 mA cm^{-2} and 778 mV respectively was seen and a FF of 56.0%. The lower band gap of 1.39 eV did increase the EQE response at higher wavelengths up to 950 nm without leaving a remaining CdSe layer. Thinner films of CdSe (< 175 nm) were not thick enough to lower the band gap of CdTe effectively to increase the response at wavelengths >900 nm.

Thicker layers, greater than 340 nm, reduced the band gap of CdTe by forming the ternary compound, but left a CdSe layer that absorbed too much light to work as an effective window layer. As a result the EQE was poor across all wavelengths resulting in low Jsc values.

Further work will focus on increasing the deposition rate and improving the homogeneity of the CdSe thin film to increase the efficiency of the complete CdTe device. The chemical bath will also be investigated as a route to deliver dopants into the CdTe layer to further improve device efficiency.

REFERENCES

[1] M. Green et al., "Solar cell efficiency tables (Version 53)", *Progress in Photovoltaics: Research and Applications*, vol. 27, no. 1, pp. 3-12, 2018.

[2] S. Rühle, "Tabulated values of the Shockley–Queisser limit for single junction solar cells", *Solar Energy*, vol. 130, pp. 139-147, 2016.

[3] R. Geisthardt, M. Topic and J. Sites, "Status and Potential of CdTe Solar-Cell Efficiency", *IEEE Journal of Photovoltaics*, vol. 5, no. 4, pp. 1217-1221, 2015.

[4] Z. Feng et al., "Raman, infrared, photoluminescence and theoretical studies of the II-VI-VI ternary CdSeTe", *Journal of Crystal Growth*, vol. 138, no. 1-4, pp. 239-243, 1994.

[5] J. Kephart et al., "Sputter-Deposited Oxides for Interface Passivation of CdTe Photovoltaics", *IEEE Journal of Photovoltaics*, vol. 8, no. 2, pp. 587-593, 2018.

[6] J. Poplawsky et al., "Structural and compositional dependence of the $CdTe_xSe_{1-x}$ alloy layer photoactivity in CdTe-based solar cells", *Nature Communications*, vol. 7, no. 1, 2016.

[7] T. Baines et al., "Incorporation of CdSe layers into CdTe thin film solar cells", *Solar Energy Materials and Solar Cells*, vol. 180, pp. 196-204, 2018.

[8] N. Paudel and Y. Yan, "Enhancing the photo-currents of CdTe thin-film solar cells in both short and long wavelength regions", *Applied Physics Letters*, vol. 105, no. 18, p. 183510, 2014.

[9] S. Ninomiya and S. Adachi, "Optical properties of cubic and hexagonal CdSe", *Journal of Applied Physics*, vol. 78, no. 7, pp. 4681-4689, 1995.

[10] A. Munshi et al., "Polycrystalline CdSeTe/CdTe Absorber Cells With 28 mA/cm^2 Short-Circuit Current", *IEEE Journal of Photovoltaics*, vol. 8, no. 1, pp. 310-314, 2018

[11] D. Swanson, J. Sites and W. Sampath, "Co-sublimation of $CdSe_xTe_{1-x}$ layers for CdTe solar cells", *Solar Energy Materials and Solar Cells*, vol. 159, pp. 389-394, 2017.

[12] K. Chopra and S. Das, *Thin film solar cells*. New York: Plenum Pr, 1983.

[13] S. Kamble, A. Sikora, S. Pawar, N. Maldar and L. Deshmukh, "Cobalt sulfide thin films: Chemical growth, reaction kinetics and microstructural analysis", *Journal of Alloys and Compounds*, vol. 623, pp. 466-472, 2015.

[14] N. Gopakumar, P. Anjana and P. Vidyadharan Pillai, "Chemical bath deposition and characterization of CdSe thin films for optoelectronic applications", *Journal of Materials Science*, vol. 45, no. 24, pp. 6653-6656, 2010. [15] R. Kainthla, D. Pandya and K. Chopra, "Solution Growth of CdSe and PbSe Films", *Journal of The Electrochemical Society*, vol. 127, no. 2, p. 277, 1980.

[16] I. Dharmadasa, "Review of the $CdCl_2$ Treatment Used in CdS/CdTe Thin Film Solar Cell Development and New Evidence towards Improved Understanding", *Coatings*, vol. 4, no. 2, pp. 282-307, 2014.

[17] Y. Xu and W. Ching, "Electronic,optical, and structural properties of some wurtzite crystals", *Physical Review B*, vol. 48, no. 7, pp. 4335-4351, 1993.

[18] Z. Zhou et al., "$CuInS_2$ quantum dot-sensitized TiO_2 nanorod array photoelectrodes: synthesis and performance optimization", *Nanoscale Research Letters*, vol. 7, no. 1, p. 652, 2012.

[19] J. Tauc, "Optical properties and electronic structure of amorphous Ge and Si", *Materials Research Bulletin*, vol. 3, no. 1, pp. 37-46, 1968.